Image De-Noising and Micro Crack Detection of Solar Cells

Zeinab Mahdavipour

1- PhD Graduate, School of Electrical and Electronic Engineering, Engineering Campus,*Universiti Sains Malaysia*, 14300 Penang, Malaysia.
z.mahdavipour@yahoo.co.uk

Abstract:

Solar cell is known as a sustainable and environment friendly source of energy in nature. It converts sunlight directly into electricity with zero emission and also without side-effects on the environment. But, solar cells have optical and mechanical defects which include the type of micro crack, the size of crack, and the noise from electrical or electromechanical interference during the image acquisition. This paper through image processing techniques presents several groups of methods to compare between two types of solar cell images, which are from solar cells with crack and without crack. In the first step, there are some methods such as Gaussian filter, Diffusion filter, Wavelet filter; Fast Fourier Transform and notch filter to de-noise images. In the next level, the study presents Gray Level Co-occurrence Matrix (GLCM) method to feature extraction of images and also the Hough transform to perform crack detection and analysis. Finally, the results confirm that the image from the solar cell with crack has the highest "S" measure compared to good images which have lower "S" measure levels.

1. Introduction

Solar cells are known as one of the most hopeful candidates to have sustainable, environmentally friendly energy sources which are able to convert sunlight directly to electric power and without having any bad effect to the natural environment [1]. In fact, Solar cells which convert the photons from the sun to electricity are mostly based on crystalline silicon in the recent market. It can produce a good performance in its usable lifespan and provide conversion efficiency between the currently available methods [2, 28].

But, the solar cells have various deficiencies which are recognized as "micro-crack" and "noise spectroscopy". For example, a micro crack arises due to the mechanical category and also can be categorized according to types and sizes [2]. In addition, solar cells are fragile, which can be a reason of the decreased yield during processing. It may cause electrical failure in the post processing stages of solar cells and solar modules too [3]. As noted above, one of the solar cell's defects is noise, which has various types such as thermal, shot, generation, and recombination. In fact, low frequency noise is a more sensitive tool for analysing the degradation phenomena, like electro migration and that sort of breakdown. All types of noise play a different role in the reliability analysis [24].

In turn, micro cracks as another type of a solar cell defect are known. In recent years, using visual images to detect micro-cracks of solar cells and wafers are presented to improve the efficiency and also the detecting time. Moreover, through the methods of the smoothing process, micro cracks will be detected in solar cells precisely in the similar thickness. Also, a novel checking system combining a tunable exposing unit to inspect micro-cracks of solar wafers is recommended. With the infrared ray transmitting through silicon wafers, the inspecting images will be captured by a CCD camera, and the micro-crack defects from the images will appear quite clear. Therefore, to distinguish either micro-cracks or grain boundaries from the images, this can be done precisely and also easily by definite algorithms. This inspecting system is particularly efficient when the thickness of the multi-crystalline silicon wafer is not constant. Overall, it is safe to say that there are a lot of studies which suggested for the inspecting methods to detect solar cell defects, like the image processing scheme for crack detection [3].

According to the cracks' sizes, they can be grouped as either macro or micro cracks (μ-cracks). For example, a crack with a size smaller than 30 μm in width is usually grouped, as a micro crack. In turn, cracks can be classified as either visible or invisible too. The visible cracks happen on the surface of a silicon cell depending on their sizes, which may or may not be seen by naked eyes. The invisible internal defects can be detected by using near-infrared (NIR) imaging technologies [4]. As an example, "Fig. 1"
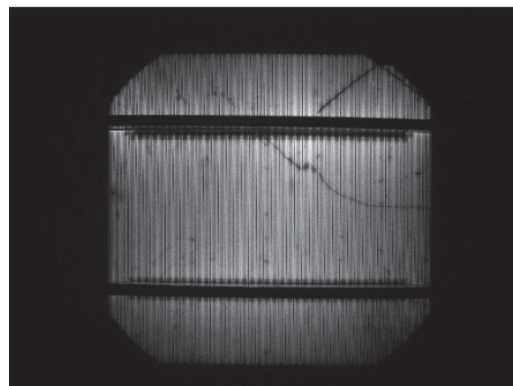

Fig.1. A solar cell image with micro crack and noise

shows a solar cell image which includes micro crack and noise.

In turn, there are various methods to detect cracks, which can be divided to two parts, the old and new methods. There are some methods which are considered as old, to reveal the cracks, such as direct sound, radiation (e.g. X-ray, gamma-ray, neutron, etc.), heat, or light into test objects and observe their responses. Other common methods for crack inspection include the dye inspection, eddy current inspection [6], acoustic inspection [7, 8] ultrasonic inspection [9], radiant heat thermography (RHT) [10, 11] scanning acoustic microscopy (SAM) [12, 13], photoluminescence (PL) [14, 15], electroluminescence (EL) [16, 17], resonance ultrasonic vibration (RUV) [18, 19], electronic speckle pattern interferometer (ESPI) [20], and Micro crack detection of multi-crystalline silicon solar wafer using machine vision techniques [4].

This paper will compare two groups of images of solar cells with crack and without crack by the image processing techniques. These methods include image enhancement via, Gaussian, Diffusion, Wavelet, and Notch filters. Meanwhile, the Hough transform was used for crack detection.

2. De-noising Images by Different Filters

Digital images are prone to diverse types of noises [29]. Noises are the outcome of faults in the image attainment process that would result in pixel values which do not reflect the real intensities of the true scene. There are several ways which noise can be presented into an image, depending on how the image is captured [22, 25]. For instance, in acquiring images with a CCD camera, factors affecting the amount of noise in the resulting image are light levels and sensor temperature. In turn, the periodic noise in an image rises typically from electrical or electromechanical interference during the image acquisition, which has been filtered by notch filter and wavelet filter [22, 25]. In this paper, the images are obtained directly in a digital format as a CCD detector which can create

۵۶

noise. The images are captured at a spatial resolution of 640×480 pixels.

2.1. Diffusion Filter

The diffusion filter as a high pass filter is used to de-noise the images. In the diffusion equation structure of looking at scale-space, the diffusion coefficient $c(x, y, t)$ is supposed to be a constant independent of the space location. The anisotropic diffusion attempts to avoid the blurring effect of the Gaussian by convolving the image. The anisotropic diffusion equation is given by [21]:

$$It = div\ (c\ (x, y, t)\ \nabla I)\ =\ c(x, y. t)\ \Delta I\ +\ \nabla c.\nabla I \quad (1)$$

Where, the div is the divergence operator which with ∇ and Δ respectively are the gradient and Laplacian operators, with respect to the space variables and also I in this variable identifies the image. The function of gradient is given by [21]:

$$c(x, y, t) = g(\|\nabla I(x, y, t)\|) \quad (2)$$

There are two options available:

Option1: $\quad g\ (\nabla I) = e^{((-(\|\nabla I\|/k)2))} \quad (3)$

Option2: $\quad g(\ \nabla I) = 1/(1 + (\|\nabla I\|/k)2) \quad (4)$

2.2 Gaussian Filter

The Gaussian filter, which smoothens the whole image irrespective of its edges or details, is a local and linear filter [26]. In this study, the Gaussian as a high pass filter is used as a second filter. The transfer function of the Gaussian high pass filter is given by:

$$H(u, v) = 1 - e^{-D^2(u,v)/2D0^2} \quad (5)$$

where D_0 is a distance from the center of the frequency rectangle and $D\ (u, v)$ is the space between a point (u, v) in the frequency domain and the middle of the frequency rectangle that is given by:

$$D(u, v) = [\ (u - M/2)^2 + (v - N/2)^2]^{1/2} \quad (6)$$

where the size of image is $M \times N$ and $u = 0,1,2, ..., M - 1$, $v = 0,1,2, ..., N - 1$ [22].

2.3 Wavelet Filter

The third filter which is a Wavelet filter is used to remove noises from images where Wavelet transforms are based on small waves that are called wavelets. To perform the Wavelet transforms in two-dimensional, a two-dimensional scaling function, $\emptyset(x, y)$ and three

two-dimensional wavelets, $\varphi^H(x, y), \varphi^V(x, y)$ and $\varphi^D(x, y)$ are required. These wavelets measure functional variations-intensity variations for images along different directions. For example $\varphi^H(x, y)$, measures variations along columns (Horizontal), and also $\varphi^V(x, y)$ measures variations along rows (Vertical), and $\varphi^D(x, y)$ is for Diagonal parameters [22]. The scaled and translated functions are defined by:

$$\emptyset j, m, n(x, y) = 2^{j/2}\emptyset(2^j x - m, 2^j y - n) \quad (7)$$

$$\varphi^i j, m, n(x, y) = 2^{j/2}\varphi^i(2^j x - m, 2^j y - n) \quad (8)$$

Where, index i is the directional wavelet $i = \{H, V, D\}$, $j_0 = 0$ and $m = n = 0,1,2,…,2^\wedge j - 1$ so that $j = 0,1,2,…, j - 1$. The discrete wavelet transform (DWT) of image $f(x, y)$ of size $M \times N$ is given by [21]:

$$W_\emptyset(j_0, m, n) = \frac{1}{\sqrt{MN}} \sum_{x=0}^{M-1}\sum_{y=0}^{N-1} f(x, y)\emptyset_{j_0,m,n}(x, y) \quad (9)$$

$$W_\varphi^i(j, m, n) = \frac{1}{\sqrt{MN}} \sum_{x=0}^{M-1}\sum_{y=0}^{N-1} f(x, y)\varphi^i_{j,m,n}(x, y) \quad (10)$$

Where, $i = \{H, V, D\}$, and j_0 is an arbitrary starting scale and an approximation of $f(x, y)$ at scale j_0 is defined by $W_\emptyset(j_0, m, n)$ coefficients and also for scales $j \geq j_0$ the $W_\varphi^i(j, m, n)$ coefficients add horizontal, vertical, and diagonal details. Normally $j_0 = 0$ and $N = M = 2^J$ so that $j = 0,1,2,…, j - 1$ and $m = n = 0,1,2,…, 2^j - 1$ [22].

The common wavelet-based methods to de-noise the images are explained in the coming steps:

a) Select a wavelet (Haar) and the number of levels (scales) for the decomposition. Then calculate the FWT/DWT of the noisy image. The Haar filter coefficients are given by [22]:

$$(n) = \{1/\sqrt{2}, 1/\sqrt{2}\} \quad (11)$$

$$(n) = \{1/\sqrt{2}, -1/\sqrt{2}\} \quad (12)$$

b) Thresholding of the detail coefficients includes hard thresholding or soft thresholding. Hard thresholding means putting to zero the elements whose absolute values are lower than the threshold, and soft thresholding includes first setting to zero the elements whose absolute values are lower than the threshold and then scaling the nonzero coefficients to ward zero [22].

c) Calculating the inverse wavelet transforms is by using the original approximation coefficients [22].

"Fig. 2" shows the crack image and the good image in all situations before and after de-noising by different filters.
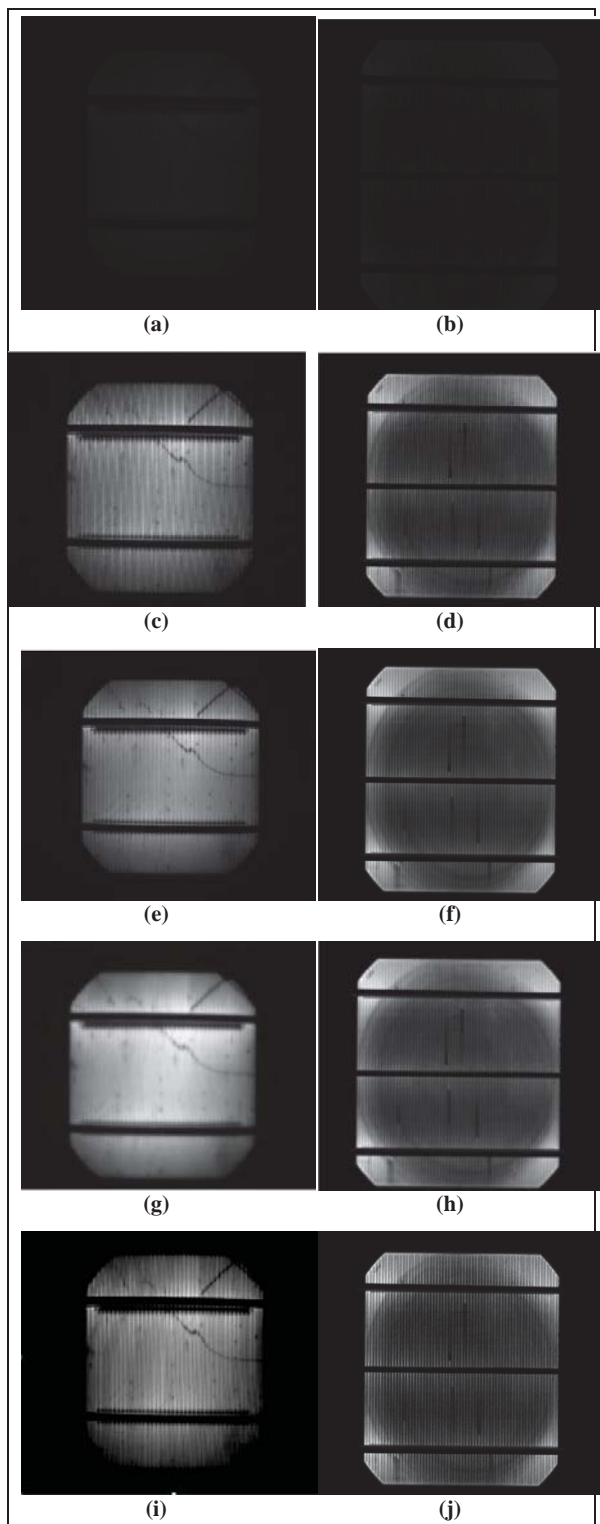
Fig.2. (a) Original Crack image, (b) Original Good image, (c) Crack image enhancement, (d) Good image enhancement, (e) Crack image after using diffusion filter, (f) Good image after using diffusion filter, (g) Crack image after using Gaussian filter, (h) Good image after using Gaussian filter, (i) Crack image after de-noising by wavelet filter, (j) Good image after de-noising by wavelet filter

After de-noising images with Diffusion, Gaussian, and Wavelet filter, we compared the feature extraction properties with two groups of images by Gray Level Co-occurrence Matrix (GLCM) method. This method is a statistical process of inspecting structures which concerns the spatial connection of pixels. The gray-level co-occurrence matrix can display certain properties about the spatial distribution of the gray levels in the texture image, which include calculating of four factors such as Contrast, Correlation, Energy, and Homogeneity [27]. The results will be discussed in section "4".

2.4 Fast Fourier Transform (FFT) and Notch Filter

In this subsection, de-noising images are achieved by two (2) dimensional FFT (Fast Fourier Transform) which is given in the following equation to calculate by:

$$f(u,v) = \frac{1}{MN} \sum_{x=0}^{M-1} \sum_{y=0}^{N-1} f(x,y) e^{-2\pi j\left(\frac{ux}{M}+\frac{vy}{N}\right)} \quad (13)$$

where $M \times N$ is size of image and $u = 0,1,2,\ldots,M-1, v = 0,1,2,\ldots,N-1$ [22].

The next step after using Fast Fourier Transform 2-D FFT is using a notch filter which is a low pass filter to de-noise the images. A notch filter rejects or passes frequencies in a predefined neighbourhood, at the middle of the frequency rectangle which is defined by the following equation:

$$D(u,v) = [\,(u-M/2)^2 + (v-N/2)^2]^{1/2} \quad (14)$$

where $D(u,v)$ is the distance between a point (u,v) in a frequency domain and middle of the frequency rectangle. The following equation to calculate notch filter is shown by [23]:

$$H(u,v) = \begin{cases} 0 \ if \ D_0 - \frac{W}{2} \le D \le D_0 + \frac{W}{2} \\ 1 \qquad\qquad otherwise \end{cases} \quad (15)$$

where a cut off frequency is D_0, D is the distance, and $D(u,v)$ is from the middle of the filter, and W is the width of the band and $M \times N$ is the size of images. The distance computations for each filter are D_k and D_{-k}, which are defined in the following equations:

$$D_k(u,v) = [(u - M/2 - u_k)^2 + (v - N/2 - v_k)^2]^{1/2} \quad (16)$$

$$D_{-k}(u,v) = [(u - M/2 + u_k)^2 + (v - N/2 + v_k)^2]^{1/2} \quad (17)$$

where $(M/2, N/2)$ is the centre of the frequency rectangle and k is notch pairs and $u = 0,1,2,\ldots,M-1, v = 0,1,2,\ldots,N-1$. The following equation to calculate notch filter is shown by [24]:

$$H_N(u,v) = \prod_{k=1}\left[\frac{1}{1 + [D_{0k}/D_k(u,v)]^{2n}}\right]\left[\frac{1}{1 + [D_{0k}/D_{-k}(u,v)]^{2n}}\right] \quad (18)$$

Equation (18) is a Butterworth notch reject filter of order n, containing k notch pairs where D_k and D_{-k} are given by equations (16) and (17) and D_0 is a cut off frequency [22].

After using the notch filter, we get 2 dimensional IFFT (Inverse Fast Fourier Transform) and in the next step, wavelet filter is used to de-noise the image. At the final step, Hough transform is used to crack detection. "Fig. 3" demonstrates the crack image and the good image after using FFT (Fast Fourier Transform) and Notch filter.
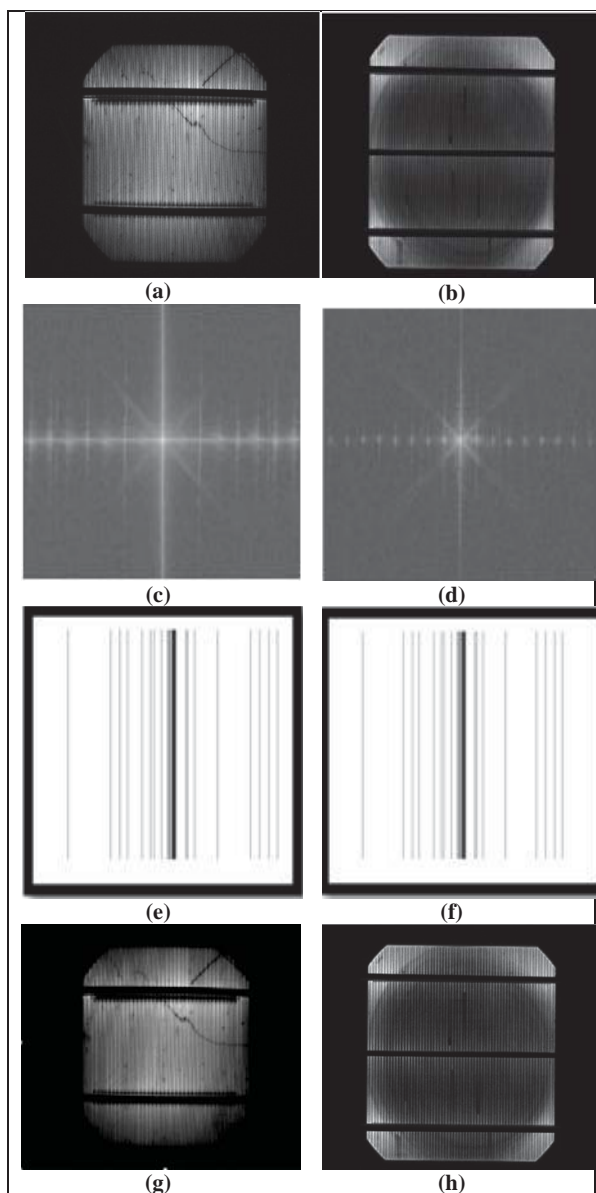
Fig.3. (a) Crack image enhancement, (b) Good image enhancement, (c) Spectrum Crack image, (d) Spectrum Good image, (e) A vertical notch filter of Crack image, (f) A vertical notch filter of Good image, (g) Crack image after de-noising by wavelet filter, (h) Good image after de-noising by wavelet filter

3. Hough Transform

Hough transform technique is a strong universal method used to fit the lines and curves. This technique recognizes a specific class of shapes based on a voting procedure that extracts a specific feature of the image. The method executes a mapping from the $x - y$ space to the $r - \theta$ space, using parameters to represent solutions of the line equation which is defined by [25]:

$$r = x \cos \theta + y \sin \theta \tag{19}$$

where (x, y) is the coordinate of a pixel, and (r, θ) is the equivalent distance-angel parameter curve. In order to extract the crack's feature in the texture image, each pixel in the original image is planned to the Hough space using all values of θ. Hence, we have a sin wave in the Hough space for each single pixel and also this is an accumulator array A, which is used to count the number of, intersects of different r and θ values. Therefore, for each image the concentricity S measure is computed by finding the maximum values of r for every angle, seen as follows [23].

$$S(\theta) = \max(A_r, \theta) \tag{20}$$

"Fig. 4" shows the Hough transform of Crack and Good images.

4. Results

In the first section, between six tested images, one of them has a crack while other images are good or so-called, intact solar cells. This part includes image enhancement by using a multi-stage process, which "Fig. 2" showed the crack image and good image in all situations before and after de-noising by different filters, which include Gaussian filter, Diffusion filter, and Wavelet filter. After filtering, feature extraction was obtained by GLCM. According to our findings, the results show that:

• The original images had low levels of contrast, while in comparison with the outcome of different filters, wavelet images had the highest contrast.

• The wavelet filter produced the highest level of variance, while the original images have the best result in terms of variance level.

"Fig. 3" as the second part of the process incorporates a Fast Fourier Transform (FFT) and Notch filter as low pass filter, Inverse Fast Fourier Transform (IFFT), and Wavelet filter. The results of Hough transform and S measure are shown in "Fig. 4". The final result is comparing the images with a crack and without a crack, as shown in "Fig. 5". The results confirm that, the image with a crack has the highest S measure compared to the good images. "Fig. 3" (a) which show crack image enhancement, (b) shows good image enhancement, (c) shows the FFT spectrum of the crack image, and (d) shows the FFT spectrum of good image.
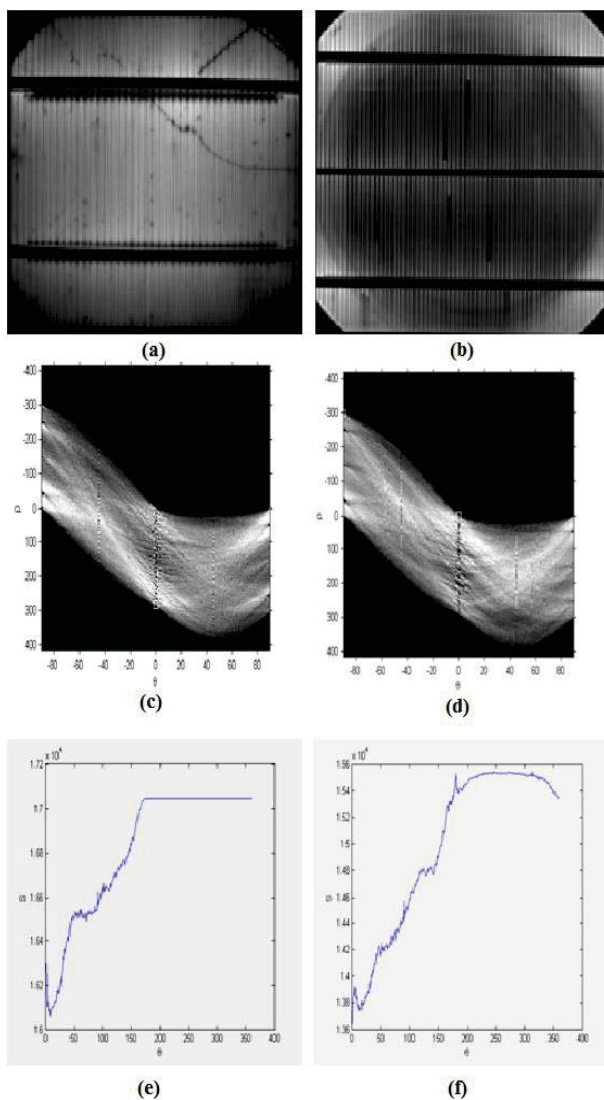
Fig.4. (a) Crack image after cropping, (b) Good image after cropping, (c) Hough transform of Crack image, (d) Hough transform of Good image, (e) S measure of Crack image, (f) S measure of Good image

• While the original images had low levels of correlation, the Gaussian filter produced the highest level of correlation compared to other filters used.

• In terms of energy, and while the original images had high levels of energy, the wavelet filter produced lower levels of energy comparatively.

• The wavelet filter produced the best result in terms of homogeneity level.

• In terms of dissimilarity, while the original images have the lowest level of dissimilarity, the wavelet filter produced the highest level of dissimilarity comparatively.

• While the original images have the lowest level of entropy, in comparison with the consequence of different filters, wavelet images have the highest level of entropy.

The vertical axis in "Fig. 3" (c) and (d) reveals a series of small bursts of energy which correspond to the nearly sinusoidal connection [22]. Also in (e) and (f), they show the vertical notch filter of the crack image and good image, (g) shows the crack image after using Wavelet filter, and (h) shows the good image after de-noising by the Wavelet filter.

We have gotten the cropped image before Hough transform for crack detection and finally for comparing the crack and good images. "Fig. 4" (a), (b) are cropped images after using the Wavelet filter, (c) illustrates result from Hough transform for crack image, (d) shows result from Hough transform for good image, (e) and (f) show the result of "S" measures for crack and good images graphically, respectively.

5. Conclusion

The main focus in this paper is to compare the various images processing techniques to de-noise the solar cell images. Different filters such as diffusion filter, wavelet filter and gaussian filter have beeng investigated. Features extraction of images was achieved by Gray Level Co-occurrence Matrix.

The second part of this study includes image enhancement by using a multi-stage process. This process incorporated a Fast Fourier Transform (FFT), low pass filter (LPF) notch filter, IFFT, and Wavelet filter. Then, the Hough transform and "S" measure were performed. Finally, the result is compared, between the images with a crack and without a crack. The result showed that the image with a crack had the highest "S" measure compared to the good images, which had lower levels.
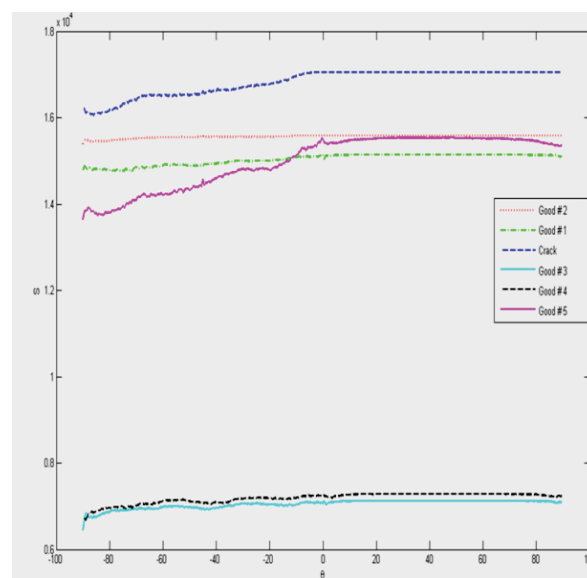
Fig.5. S measures for comparison.

Acknowledgment

I would like to extend my appreciation to my supervisor, Professor Dr Mohd Zaid Abdullah who has inspired and accompanied me throughout my study. I really appreciate as well the sacrifice of my wonderful husband Dr. Aria Hajjafari for his support, understanding, and encouragement.

References

[1] V. Meemongkolkiat, "Development of high efficiency monocrystalline silicon solar cells trough improvement optical and electrical confinement" Ph.D thesis, Georgia Institute of Technology, pp. 1-6, 2008.

[2] C.G. Zimmermann, "The impact of mechanical defects on the reliability of solar cells in aerospace applications" IEEE Transactions on Device and Materials Reliability, vol. 6, no. 3, pp. 486-494, 2006.

[3] S. Sheng Ke, K. Wei Lin, Y. Cheng Lin, J. Ting Chen, , Y. Hsing Wang and C. Sheng Liu, "High-performance Inspecting System for Detecing Micro-crack Defect of Solar Wafer" IEEE International Congress on Image and Signal Processing, pp. 494-497, 2010.

[4] Y.C. Chiou, and L. Liang, "Micro crack detection of multi-crystalline silicon solar wafer using machine" Sensor Review, Emerald Group Publishing Limited [ISSN 0260-2288], vol. 31: pp. 154-165, 2011.

[5] P. R. a. B. Sopori, "Strength of Si Wafers with Micro cracks": A Theoretical Model, in 33rd IEEE Photovoltaic Specialists Conference. 2008, IEEE: San Diego, California, pp. 1-7, 2008.

[6] G. Zenzinger, J. Bamberg W. Satzger and V. Carl, "Thermographic Crack Detection by Eddy Current Excitation" Nondestructive Testing and Evaluation", vol.22, pp. 101-11, 2007.

[7] C. Hilmersson, D.P. Hess, W. Dallas, S. Ostapenko, Crack detection in single-crystalline silicon wafers using impact testing Elsevier, vol.66, no.8, pp. 755-60, 2008.

[8] K. Yagi, H. Kanishi, and Y. Kawagoe, "Substrate crack inspection method, substrate crack inspection apparatus, and solar battery module manufacturing method", US Patent 7,191,656 B2, 2007.

[9] K. Reber, M. Beller "Ultrasonic in-line inspection tools to inspect older pipelines for cracks in girth and long-seam welds", Pigging Products and Services Association,, www.ppsa-online.com/papers/, 2003.

[10] M. Pilla, F. Galmiche, and X. Maldague, "Thermographic inspection of cracked solar cells" Proceedings of SPIE, vol. 4710, pp.699-703, 2002.

[11] J. W. Devitt, E. Bantel, J.M. Sparks, and J.S. Kania "Apparatus and method for detecting fatigue cracks using infrared thermography", US Patent 5, 111,048, 1992.

[12] D. Knauss, T. Zhai, G.A.D. Briggs, and J.W. Martin, "Measuring short cracks by time-resolved acoustic microscopy" Advances in Acoustic Microscopy, vol. 1, pp. 49-77, 1995.

[13] Z. M. Connor, M.E. Fine, J.D. Achenbach, and M.E. Seniw, "Using scanning acoustic microscopy to study subsurface defects and crack propagation in materials" Journal of Microscopy, vol.50, no. 11, 1998.

[14] T. Trupke, R.A. Bardos, M.C. Schubert, and W. Warta, "Photoluminescence imaging of silicon wafers" Applied Physics Letter, vol. 89, no .4, pp. 044107, 2006a.

[15] T.Trupke, R.A. Bardos, M.D. Abbott, F.W. Chen, J.E. Cotter, and A. Lorenz, "Fast photoluminescence imaging of silicon wafers" Proceedings of the 4thWCPVSEC,. Waikoloa, HI, USA, pp. 928-931, 2006b.

[16] T. Fuyuki, T. Yamazaki, Y. Takahashi, and Y. Uraoka "Photographic surveying of minority carrier diffusion length in polycrystalline silicon solar cells by electroluminescence" Applied Physics Letter Electronic Transport And Semiconductors, vol. 86, no.26, pp.262108, 2005.

[17] F. Dreckschmidt, T. Kaden, H. Fiedler, and H.J. Mo¨ller,"Electroluminescence investigation of the decoration of extended defects in multicrystalline silicon" Proceedings of the 22nd European Photovoltaic Solar Energy Conference,. Milan, Italy, pp. 283-286, 2007.

[18] O. Polupan and S. Ostapenko "Theoretical modeling of full-size silicon wafers with micro cracks for the purpose of defect diagnostics", REU Symposium, University of South Florida, Tampa, FL, April 6, 2006.

[19] W. Dallas, O. Polupan, and S. Ostapenko, "Resonance ultrasonic vibrations for crack detection in photovoltaic silicon wafers" Measurement Science and Technology, vol.18,no.3, pp. 852-858, 2008.

[20] T. K. Wen, C.C. Yin, "Crack detection in photovoltaic cells by interferometric analysis of electronic speckle patterns" Elsevier 98(Solar Energy Materials and Solar Cells), vol. 98, pp. 216-223, 2011.

[21] P. Perona, J. Malik "Scale-space and edge detection using anisotropic diffusion" IEEE Transactions on Pattern Analysis and Machine Intelligence, vol. 12, pp. 629–639,1990.

[22] R.C. Gonzalez and R.E. Woods, "Digital image processing" United States of America: Pearson Education, Inc, 2010.

[23] S. Nashat, A. Abdullah, and M.Z. Abdullah (2011) "A Robust Crack Detection Method for Non-uniform Distributions of Coloured and Textured Image" IEEE International Conference on Imaging Systems and Techniques IST. Malaysia.

[24] P. Koktavy, J. Vanek, Z. Chobola, K. Kubickova, and J. Kazelle, "Solar Cells Noise Diagnostic and LBIC Comparison", AIP Conference Proceedings, pp. 306-309, 2007.

[25] P. Subashini and M. Krishnaveni" Image Denoising Based on Wavelet Analysis for Satellite Imagery", Advances in Wavelet Theory and Their Applications in Engineering, Physics and Technology, Dr. Dumitru Baleanu (Ed.), ISBN: 978-953-51-0494-0, InTech, 2012.

[26] B. K. Shreyamsha Kumar," Image de-noising based on gaussian/bilateral filter and its method noise thresholding", Signal, Image and Video Processing, vol.7, no. 6, pp. 1159-1172, 2013.

[27] D. GADKARI, "Image Quality Analysis Using GLCM" Msc. thesis, University of Central Florida,Orlando, Florida, pp. 8-16, 2004.

[28] Y. Mei, J.S. Mitchell, G. Roientan Lahiji and K. Najafi, "Wafer Bonding Technology For Vacuum Packaging Using Gold silicon Eutectic", Journal of Iranian Association of Electrical and Electronics Engineers, vol.1, no.2, Summer & Fall, 2004.

[29] R. Kamran, H. Nezamabadi and S. Saryazdi, " A Large Scale Image In painting Method Based on Image Decomposition to Texture and Structure Sub-Images", Journal of Iranian Association of Electrical and Electronics Engineers, vol.8, no.2, Fall & Winter 2011.